A general well-balanced finite volume scheme for Euler equations with gravity

Jonas Berberich, Praveen Chandrashekar, Christian Klingenberg

Abstract We present a second order well-balanced Godunov-type finite volume scheme for compressible Euler equations with a gravitational source term. The scheme is designed to work for any hydrostatic equilibrium, which must be known á priori. It can be combined with any numerical flux function, time-stepping method, and grid topology. The scheme is based on the reconstruction of a special set of variables and a special source term discretization. We show the well-balanced property numerically for isothermal and polytropic equilibria in one and two dimensions using the Roe flux function and an explicit three-stage Runge–Kutta scheme. We demonstrate the superior resolution of small pressure perturbations of hydrostatic equilibria, down to an order 10^{-10} and below compared to the hydrostatic background.

1 Introduction

Astrophysical processes involve many orders of magnitude in space, time and thermodynamical quantities such as density and pressure. The overall evolution of our sun for example can be measured in a scale of 10^{10} years, but from a hydrodynamical point of view, the sun can be seen as being in a hydrostatic equilibrium locally in time. Many hydrodynamical processes are small perturbations to that equilibrium. It is common to model these dynamics using compressible Euler equations with gravity. The astrophysical equation of states are very complex since they take into

Jonas Berberich
Dept. of Mathematics, Univ. of Würzburg, Germany, e-mail: jonas.berberich@slh-code.org

Praveen Chandrashekar
TIFR Center for Applicable Mathematics, Bangalore, India, e-mail: praveen@tifrbng.res.in

Christian Klingenberg
Dept. of Mathematics, Univ. of Würzburg, Germany, e-mail: klingenberg@mathematik.uni-wuerzburg.de

account a whole bunch of physical effects including relativistic and quantum effects. Typically, there is no closed formulation for these equations of state. Hence, one can not hope to calculate the hydrostatic equilibria analytically. Also, many processes occur at low Mach numbers that require special schemes. It is also necessary to use general grids in order to be able to compute flows inside star-like geometry where Cartesian grids may not be suitable.

In this paper such a general well-balanced finite volume scheme will be presented which can preserve hydrostatic solutions exactly on even coarse meshes. It is designed to balance any arbitrary hydrostatic equilibrium, even if it is only given numerically on the grid. Thus it can cope with arbitrary equations of state. It can be combined with any numerical flux function including low Mach number fluxes. Also, any time-stepping method can be used including implicit methods. We will present the scheme for one spatial dimension, but it can be easily extended to two or three spatial dimensions. In numerical simulations it can be practical to use non-Cartesian grids, which can be mapped to a Cartesian grid, to reflect the systems symmetries. Our scheme can be used on this kind of grid also. Numerical results are presented to show the well-balanced property and also the ability of the scheme to accurately resolve small perturbations around the hydrostatic solution.

2 1-D Euler Equations with Gravity

Consider the system of compressible Euler equations in one dimension which models conservation of mass, momentum and energy and is given by

$$\begin{aligned} \frac{\partial \rho}{\partial t} + \frac{\partial}{\partial x}(\rho u) &= 0, \\ \frac{\partial}{\partial t}(\rho u) + \frac{\partial}{\partial x}(p + \rho u^2) &= -\rho \frac{\mathrm{d}\phi}{\mathrm{d}x}, \\ \frac{\partial E}{\partial t} + \frac{\partial}{\partial x}(Eu + pu) &= 0. \end{aligned}$$

Here ρ is the density, u is the velocity, p is the pressure, E is the energy per unit volume including the gravitational energy and ϕ is the gravitational potential. The total energy E is given by $E = \rho\varepsilon + \frac{1}{2}\rho u^2 + \rho\phi$ where ε is the internal energy per unit mass. We can write the above set of coupled equations in a compact notation as

$$\frac{\partial \boldsymbol{q}}{\partial t} + \frac{\partial \boldsymbol{f}}{\partial x} = \begin{bmatrix} 0 \\ s \\ 0 \end{bmatrix}, \qquad s = -\rho \frac{\mathrm{d}\phi}{\mathrm{d}x}$$

where $\boldsymbol{q}$ is the set of conserved variables and $\boldsymbol{f}$ is the corresponding flux vector.

2.1 Hydrostatic States

Consider the hydrostatic stationary solution, i.e., for which the velocity is $\bar{u} = 0$. In this case, the mass and energy conservation equations are automatically satisfied. The momentum equation becomes an ordinary differential equation given by

$$\frac{\mathrm{d}\bar{p}}{\mathrm{d}x} = -\bar{\rho}\frac{\mathrm{d}\phi}{\mathrm{d}x}. \tag{1}$$

We will write the hydrostatic solution as

$$\bar{\rho} = \rho_0\alpha(x), \qquad \bar{p} = p_0\beta(x),$$

where p_0, ρ_0 are reference values at some location $x = x_0$ and $\alpha(x)$, $\beta(x)$ are non-dimensional functions. These functions must satisfy the hydrostatic equation (1)

$$p_0\beta'(x) = -\rho_0\alpha(y)\phi'(x), \qquad \text{i.e.,} \qquad \phi'(x) = -\frac{p_0}{\rho_0}\frac{\beta'(x)}{\alpha(x)}, \tag{2}$$

Note that since the pressure and density are strictly positive, we have $\alpha(x) > 0$, $\beta(x) > 0$.

3 1-D Finite volume scheme

Let us divide the domain into N finite volumes each of size Δx. The i'th cell is given by the interval $(x_{i-\frac{1}{2}}, x_{i+\frac{1}{2}})$. Consider the semi-discrete finite volume scheme for the i'th cell

$$\frac{\mathrm{d}\boldsymbol{q}_i}{\mathrm{d}t} + \frac{\hat{\boldsymbol{f}}_{i+\frac{1}{2}} - \hat{\boldsymbol{f}}_{i-\frac{1}{2}}}{\Delta x} = \begin{bmatrix} 0 \\ s_i \\ 0 \end{bmatrix}, \tag{3}$$

where $\hat{\boldsymbol{f}}_{i+\frac{1}{2}} = \hat{\boldsymbol{f}}(\boldsymbol{q}^L_{i+\frac{1}{2}}, \boldsymbol{q}^R_{i+\frac{1}{2}})$ is a consistent numerical flux. For the source term, we make use of the representation of the gravitational potential in terms of the hydrostatic functions α, β given by (2), and we will write the source term in the general case as

$$s(x,t) = \frac{p_0}{\rho_0}\frac{\beta'(x)}{\alpha(x)}\rho(x,t).$$

Applying a central difference discretization to the source term, we obtain

$$s_i = \frac{p_0}{\rho_0}\frac{\beta_{i+\frac{1}{2}} - \beta_{i-\frac{1}{2}}}{\Delta x}\frac{\rho_i}{\alpha_i},$$

which is a second order accurate approximation. Note that even though we could calculate the source term exactly, we use an approximation since this helps to construct the well-balanced scheme.

To obtain the states $\boldsymbol{q}^L_{i+\frac{1}{2}}, \boldsymbol{q}^R_{i+\frac{1}{2}}$ at the cell boundary which are required to calculate the numerical flux $\hat{\boldsymbol{f}}_{i+\frac{1}{2}}$, we will reconstruct the following set of variables

$$\boldsymbol{w} = [\rho/\alpha,\ u,\ p/\beta]^\top.$$

Once $\boldsymbol{w}^L_{i+\frac{1}{2}}$ etc. are computed, the primitive variables are obtained as

$$\rho^L_{i+\frac{1}{2}} = \alpha_{i+\frac{1}{2}}(w_1)^L_{i+\frac{1}{2}}, \qquad u^L_{i+\frac{1}{2}} = (w_2)^L_{i+\frac{1}{2}}, \qquad p^L_{i+\frac{1}{2}} = \beta_{i+\frac{1}{2}}(w_3)^L_{i+\frac{1}{2}}, \quad \text{etc.},$$

where $\alpha_{i+\frac{1}{2}} = \alpha(x_{i+\frac{1}{2}})$ and $\beta_{i+\frac{1}{2}} = \beta(x_{i+\frac{1}{2}})$.

3.1 Well-balanced property

We now state the basic result on the well-balanced property.

Theorem 1. *The finite volume scheme (3) together with any consistent numerical flux and reconstruction of $\boldsymbol{w}$ variables is well-balanced in the sense that the initial condition given by*

$$u_i = 0, \qquad \rho_i/\alpha_i = const, \qquad p_i/\beta_i = const, \qquad \forall\ i \tag{4}$$

is preserved by the numerical scheme.

Proof. Let us start the computations with an initial condition that satisfies (4). Since we reconstruct the variables $\boldsymbol{w}$ which are constant for a hydrostatic solution, at any interface $i+\frac{1}{2}$ we have

$$u^L_{i+\frac{1}{2}} = u^R_{i+\frac{1}{2}} = 0, \qquad \rho^L_{i+\frac{1}{2}} = \rho^R_{i+\frac{1}{2}} =: \rho_{i+\frac{1}{2}}, \qquad p^L_{i+\frac{1}{2}} = p^R_{i+\frac{1}{2}} =: p_{i+\frac{1}{2}}.$$

Since the numerical flux is consistent, we get

$$\hat{\boldsymbol{f}}_{i-\frac{1}{2}} = [0, p_{i-\frac{1}{2}}, 0]^\top, \qquad \hat{\boldsymbol{f}}_{i+\frac{1}{2}} = [0, p_{i+\frac{1}{2}}, 0]^\top.$$

The flux in mass and energy equations are zero and the gravitational source term in the energy equation is also zero. Hence the mass and energy equations are already well balanced, i.e., $\frac{\mathrm{d}\boldsymbol{q}^{(1)}_i}{\mathrm{d}t} = 0$ and $\frac{\mathrm{d}\boldsymbol{q}^{(3)}_i}{\mathrm{d}t} = 0$. It remains to check the momentum equation. On the left we have

$$\frac{\hat{\boldsymbol{f}}^{(2)}_{i+\frac{1}{2}} - \hat{\boldsymbol{f}}^{(2)}_{i-\frac{1}{2}}}{\Delta x} = \frac{p_{i+\frac{1}{2}} - p_{i-\frac{1}{2}}}{\Delta x},$$

while on the right

$$s_i = \frac{p_0}{\rho_0}\frac{\beta_{i+\frac{1}{2}} - \beta_{i-\frac{1}{2}}}{\Delta x}\frac{\rho_i}{\alpha_i} = \frac{p_0}{\rho_0}\frac{\beta_{i+\frac{1}{2}} - \beta_{i-\frac{1}{2}}}{\Delta x}\rho_0 = \frac{p_0\beta_{i+\frac{1}{2}} - p_0\beta_{i-\frac{1}{2}}}{\Delta x} = \frac{p_{i+\frac{1}{2}} - p_{i-\frac{1}{2}}}{\Delta x}$$

and hence $\frac{\mathrm{d}\boldsymbol{q}_i^{(2)}}{\mathrm{d}t} = 0$. This proves that the initial condition is preserved under any time integration scheme. □

Remark 1. This is a general result in the sense that we have not made any assumptions on the equation of state or on the type of gravitational field. It holds for any consistent numerical flux and reconstruction scheme to obtain the cell face values.

Remark 2. It is straight forward to generalize this scheme to two or three spatial dimensions using the method of lines. It is also possible to use coordinates, which can be mapped smoothly on Cartesian coordinates. We will refer to this kind of coordinates as *curvilinear coordinates*. We will use these cases later in this article for numerical tests.

4 Numerical Tests

The scheme has been implemented in the Seven League Hydro Code [6]. We use the standard Roe flux ([7]) for all numerical experiments. For time stepping we use an explicit three-stage Runge–Kutta scheme. This scheme has been proposed in [8]. It is third order in time and has the *total variation diminishing* property. An ideal gas with a gas constant $R = 1$ and a specific heats ratio of $\gamma = 1.4$ is assumed.

4.1 1-D Numerical Results

In the one dimensional tests the domain is the interval $[0,1]$. If not stated explicitly, we use Dirichlet boundaries, which are consistent with the initial condition. This is achieved by using ghost cells and keeping them constant over time.

4.1.1 Isothermal Atmosphere

A solution of the hydrostatic equation (1) for constant temperature $T = 1$ is given by

$$\bar{\rho}(x) = \bar{p}(x) = \exp(-\phi(x)). \tag{5}$$

We choose $\alpha_0 = \beta_0 = 1$ and hence $\alpha = \bar{\rho}, \beta = \bar{p}$.

We consider the three different gravitational potentials $\phi(x) = x$, $\phi(x) = \frac{1}{2}x^2$, and $\phi(x) = \sin(2\pi x)$. For the latter we use periodic boundary conditions. The errors

after a time $t = 2.0$ in L^1 norm are given in table (1). All errors are close to machine precision.

ϕ	N	v	p	ρ
x	100	1.62316e-15	1.12521e-15	1.20681e-15
	1000	1.83243e-14	1.28197e-14	1.26239e-14
$\frac{1}{2}x^2$	100	3.21800e-16	1.72085e-16	8.52651e-16
	1000	1.27564e-14	6.03995e-15	1.31585e-14
$\sin(2\pi x)$	100	1.15182e-15	5.72931e-15	3.43836e-15
	1000	3.55886e-15	3.37666e-14	1.61612e-14

Table 1: L^1 errors for the 1-d isothermal atmosphere of section 4.1.1

4.1.2 Isentropic Atmosphere

Isentropic solutions of equation (1) are of the form

$$\bar{T}(x) = 1 - \frac{\nu - 1}{\nu}\phi(x), \quad \bar{\rho} = \bar{T}^{\frac{1}{\nu-1}}, \quad \bar{p} = \bar{\rho}^{\nu} \tag{6}$$

with $\nu = \gamma$. Again, we choose $\alpha_0 = \beta_0 = 1$ and hence $\alpha = \bar{\rho}, \beta = \bar{p}$. The same tests as in section 4.1.1 are conducted and the L^1 norms of the errors are shown in table (2). All errors are close to machine precision.

ϕ	N	v	p	ρ
x	100	1.41193e-15	9.19265e-16	1.56597e-15
	1000	1.61820e-14	1.16552e-14	1.66951e-14
$\frac{1}{2}x^2$	100	1.37162e-15	5.20695e-16	2.13718e-15
	1000	1.39921e-14	7.03848e-15	1.84036e-14
$\sin(2\pi x)$	100	5.37656e-15	1.27287e-15	1.51712e-15
	1000	2.35665e-14	2.25356e-14	1.78504e-14

Table 2: L^1 errors for the 1-d isentropic atmosphere of section 4.1.2

4.1.3 Polytropic Atmosphere

Polytropic solutions of equation (1) are more general than isentropic solutions. We can write them in the form of equation (6), but with $\nu \neq \gamma$ possible. Let us use $\nu = 1.2$ following [1]. We choose $\alpha_0 = \beta_0 = 1$ and hence $\alpha = \bar{\rho}, \beta = \bar{p}$. The same

tests as in section 4.1.1 are conducted and the L^1 norms of the errors are shown in table (3). All errors are close to machine precision.

ϕ	N	v	p	ρ
x	100	1.21736e-15	9.60343e-16	1.44995e-15
	1000	1.75455e-14	1.24413e-14	1.60103e-14
$\frac{1}{2}x^2$	100	1.39958e-15	3.96350e-16	1.20570e-15
	1000	1.31861e-14	6.04949e-15	1.45129e-14
$\sin(2\pi x)$	100	3.82965e-15	1.90958e-15	1.68809e-15
	1000	1.49882e-14	1.79979e-14	8.44363e-15

Table 3: L^1 errors for the 1-d polytropic atmosphere of section 4.1.3

4.1.4 Evolution of a Small Perturbation

To study the propagation of a small perturbation from the isothermal hydrostatic equilibrium (5), we use the following initial condition:

$$\phi(x) = \frac{1}{2}x^2,\ u = 0,\ \rho = \exp(-\phi(x)),\ p(x) = \exp(-\phi(x)) + \varepsilon \exp(-100(x-\frac{1}{2})^2).$$

This setup corresponds to comparable tests in [4] and [1]. We present this test for different ε and resolutions in figure (1). We conducted the tests using our well-balanced scheme and another scheme, which is not well-balanced. The non-well-balanced scheme is described in [6] and discretizes the source term pointwise via $s_i = \rho_i g$, where $g = -\phi'$. We set this derivative explicitly.

The test results are illustrated in figure (1). In figure (1a) we see that for a large pressure perturbation with $\varepsilon = 10^{-3}$ the well-balanced and the non-well-balanced scheme give comparable results for a short time even with a coarse grid of $N = 100$ cells. When the perturbation is decreased to $\varepsilon = 10^{-5}$, the non-well-balanced scheme with the same parameters shows significant spurious effects, as we can see in figure (1b). The well-balanced scheme still shows a good result. One has to increase the number of grid cells to get a good result with the non-well-balanced scheme for the small perturbation. We can see this in figure (1c) for $N = 500$ cells. In figure (1d) we show that the result with the well-balanced scheme does not improve significantly if we increase the number of grid cells to more than $N = 100$ even for the small perturbation. Hence, using this scheme can save computational effort by reducing the necessary resolution.

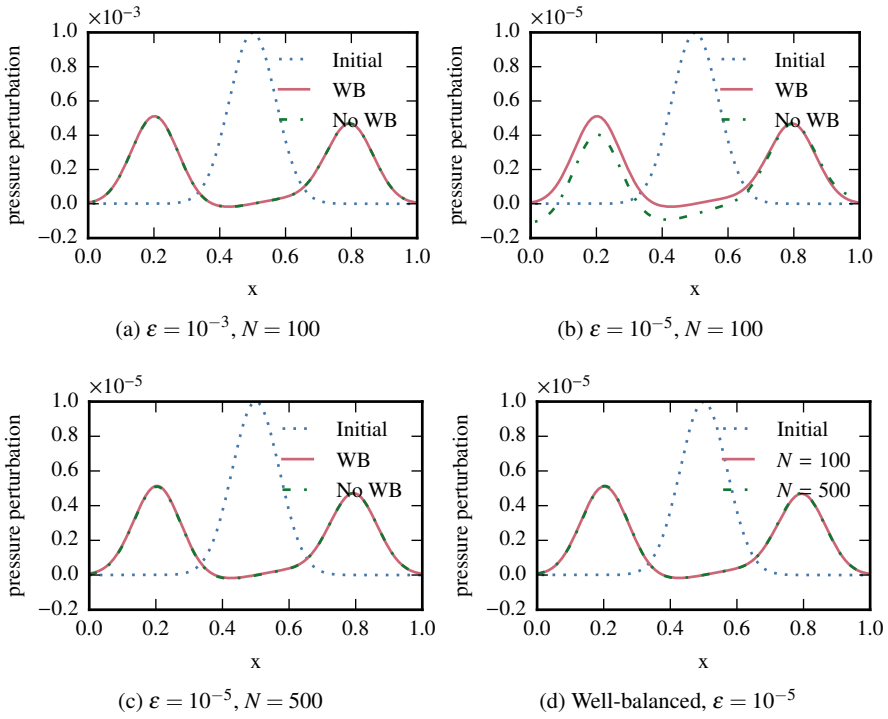

(a) $\varepsilon = 10^{-3}$, $N = 100$ (b) $\varepsilon = 10^{-5}$, $N = 100$

(c) $\varepsilon = 10^{-5}$, $N = 500$ (d) Well-balanced, $\varepsilon = 10^{-5}$

Fig. 1: Evolution of a small pressure perturbation on an 1-d isothermal equilibrium. The test setup is described in section 4.1.4

4.1.5 Non-Ideal Equation of State

In this section we aim to show the ability of the scheme to preserve hydrostatic equilibria even if an other EOS than the ideal gas EOS is used. For that, let us use the EOS for an ideal gas with radiative pressure [2]

$$p = \rho T + T^4. \tag{7}$$

Isothermal Atmosphere. With the choice of $T \equiv 1$, equation (1), and equation (7), we find an isothermal hydrostatic equilibrium given by

$$\bar{\rho}(x) = \exp(-\phi(x)), \quad \bar{p} = \exp(-\phi(x)) + 1. \tag{8}$$

With this modified EOS and equilibrium, we conduct the same tests as in section 4.1.1. The corresponding errors in L^1 norm can be seen in table (4). All errors are close to machine precision.

Polytropic Atmosphere. To derive the polytropic equilibrium shown in equation (6), the equation of state is not used. Hence, equation (6) describes an equilibrium

ϕ	N	v	p	ρ
x	100	1.05583e-15	3.74811e-15	1.80023e-15
	1000	1.53555e-14	3.19185e-14	1.31348e-14
$\frac{1}{2}x^2$	100	2.09505e-15	6.87894e-15	3.80584e-15
	1000	7.01467e-15	1.44657e-15	1.39411e-15
$\sin(2\pi x)$	100	7.01467e-15	1.44657e-15	1.39411e-15
	1000	7.01467e-15	1.44657e-15	1.39411e-15

Table 4: L^1 errors for the 1-d isothermal atmosphere with an non-ideal EOS of section 4.1.5

for every EOS. We conduct the same test as in section 4.1.3 with the EOS in equation (7) instead of an ideal gas law. The results can be seen in table (5). As in the isothermal setup, all errors stay close to machine precision.

ϕ	N	v	p	ρ
x	100	8.36066e-16	3.95795e-16	2.84772e-16
	1000	1.61427e-14	6.89920e-15	4.68958e-15
$\frac{1}{2}x^2$	100	4.37774e-16	1.26565e-16	1.07692e-16
	1000	2.71318e-15	8.31668e-16	5.95635e-16
$\sin(2\pi x)$	100	7.59499e-16	1.47105e-16	1.11022e-16
	1000	7.01467e-15	1.44657e-15	1.39411e-15

Table 5: L^1 errors for the 1-d polytropic atmosphere with an non-ideal EOS of section 4.1.5

4.2 2-D Numerical Results

The two dimensional tests will be conducted on the unit square $[0,1]\times[0,1]$. We use a Cartesian grid and the Dirichlet boundary condition, if not stated explicitly.

4.2.1 Isothermal Atmosphere

Consider the hydrostatic solution given by

$$\bar{\rho}(x,y) = \rho_0 \exp(-\rho_0\phi(x,y)/p_0), \quad \bar{p}(x,y) = p_0 \exp(-\rho_0\phi(x,y)/p_0), \qquad (9)$$

with $\phi(x,y) = x+y$, $\rho_0 = 1.21$, and $p_0 = 1$. We apply our well-balanced scheme as well as the non-well-balanced scheme to evolve this initial condition to a time $t = 1.0$.

The errors in L^1 norm with respect to the initial condition are shown in table (6). For the well-balanced scheme, all errors are close to machine precision. The non-well-balanced scheme on the other hand introduces significant errors, which decrease for the higher resolution.

cells	Scheme	v_x	v_y	p	ρ
50× 50	well-balanced	1.00232e-15	9.33272e-16	4.35663e-16	5.76417e-16
	non-well-balanced	2.55432e-03	2.55432e-03	1.71889e-03	3.82551e-03
200×200	well-balanced	2.53379e-15	2.54463e-15	1.74903e-15	1.85208e-15
	non-well-balanced	6.38199e-04	6.38199e-04	4.15871e-04	9.42026e-04

Table 6: L^1 errors for the 2-d isothermal atmosphere of section 4.2.1

4.2.2 Isentropic Atmosphere

Consider the hydrostatic solution (6) on the unit square with the gravitational potential $\phi(x,y) = x+y$. We run the simulation on different Cartesian grids to the final time $t = 1.0$. The results are shown in table (7) using the L^1 norm. Like in section 4.2.1 the well-balanced scheme keeps errors close to machine precision, while the non-well-balanced scheme introduces significant errors.

cells	Scheme	v_x	v_y	p	ρ
50× 50	well-balanced	1.09672e-15	1.01388e-15	5.44995e-16	7.99222e-16
	non-well-balanced	2.41783e-03	2.41783e-03	1.89444e-03	1.84055e-03
200×200	well-balanced	2.69286e-15	2.69081e-15	2.07824e-15	2.73340e-15
	non-well-balanced	6.11321e-04	6.11321e-04	4.63472e-04	4.50069e-04

Table 7: L^1 errors for the 2-d isentropic atmosphere of section 4.2.2

4.2.3 Polytropic Atmosphere

Consider the hydrostatic solution (6) with $\nu = 1.2$ as initial condition on the unit square with the gravitational potential $\phi(x,y) = x+y$. We run the simulation on different Cartesian grids to the final time $t = 1.0$. The results are shown in table (8) using the L^1 norm. Again, the well-balanced scheme keeps errors close to machine precision, while the non-well-balanced scheme introduces significant errors.

cells	Scheme	v_x	v_y	p	ρ
50× 50	well-balanced	1.02690e-15	1.06307e-15	5.41545e-16	6.48515e-16
	non-well-balanced	2.08336e-03	2.08336e-03	1.62272e-03	2.36791e-03
200×200	well-balanced	2.83880e-15	2.81328e-15	2.07345e-15	2.14476e-15
	non-well-balanced	5.19236e-04	5.19236e-04	3.93168e-04	5.81252e-04

Table 8: L^1 errors for the 2-d polytropic atmosphere of section 4.2.3

4.2.4 Evolution of a Small Perturbation

In this test, we study the evolution of a small perturbation added to the hydrostatic solution. We test this for the isothermal equilibrium (9) and the polytropic equilibrium (6). In correspondence with [1] and [9], we choose the same parameters as in the Sections 4.2.1 and 4.2.3 respectively and the initial pressure

$$p(x,y,0) = \bar{p}(x,y) + \eta \exp(-100\rho_0((x-0.3)^2 + (y-0.3)^2)/p_0). \qquad (10)$$

The initial density is $\rho(\cdot,\cdot,0) = \bar{\rho}$, the resolution is 64×64 cells in each test.

The results can be seen in the Figures (2) and (3). The results are similar for both equilibria: The large perturbation with $\eta = 0.1$ is well-resolved for both the well-balanced and the non-well-balanced scheme. When the perturbation is decreased to $\eta = 0.001$, the non-well-balanced scheme is not able to resolve it well anymore since the discretization errors of the background start to dominate after some time. The well-balanced scheme shows no problems for the smaller perturbation. The isothermal test case has also been conducted on a curvilinear mesh. The structure of this mesh is shown in figure (2f). The result of the test can be seen in figure (2e). We see, that the usage of the curvilinear mesh introduces no significant errors in this test. In Figures (3e) and (3f) we can see that even a small perturbation of $\eta = 10^{-10}$ or below leads to a well-resolved result, if the well-balanced scheme is used.

References

1. Chandrashekar, P. and Klingenberg, C., 2015. A second order well-balanced finite volume scheme for Euler equations with gravity. SIAM Journal on Scientific Computing, 37(3), pp.B382-B402.
2. Chandrasekhar, S., 1958. An introduction to the study of stellar structure (Vol. 2). Courier Corporation.
3. Hosea, M., Shampine, L. 1996, Applied Numerical Mathematics, 20, 21 , method of Lines for Time-Dependent Problems
4. LeVeque, R.J. and Bale, D.S., 1999. Wave propagation methods for conservation laws with source terms. In Hyperbolic problems: theory, numerics, applications (pp. 609-618). Birkhuser Basel.
5. Liou, M.-S. 2006, Journal of Computational Physics, 214, 137
6. Miczek, F. 2013, PhD thesis, Technische Universität München
7. Roe, P. 1981, Journal of Computational Physics, 43, 357

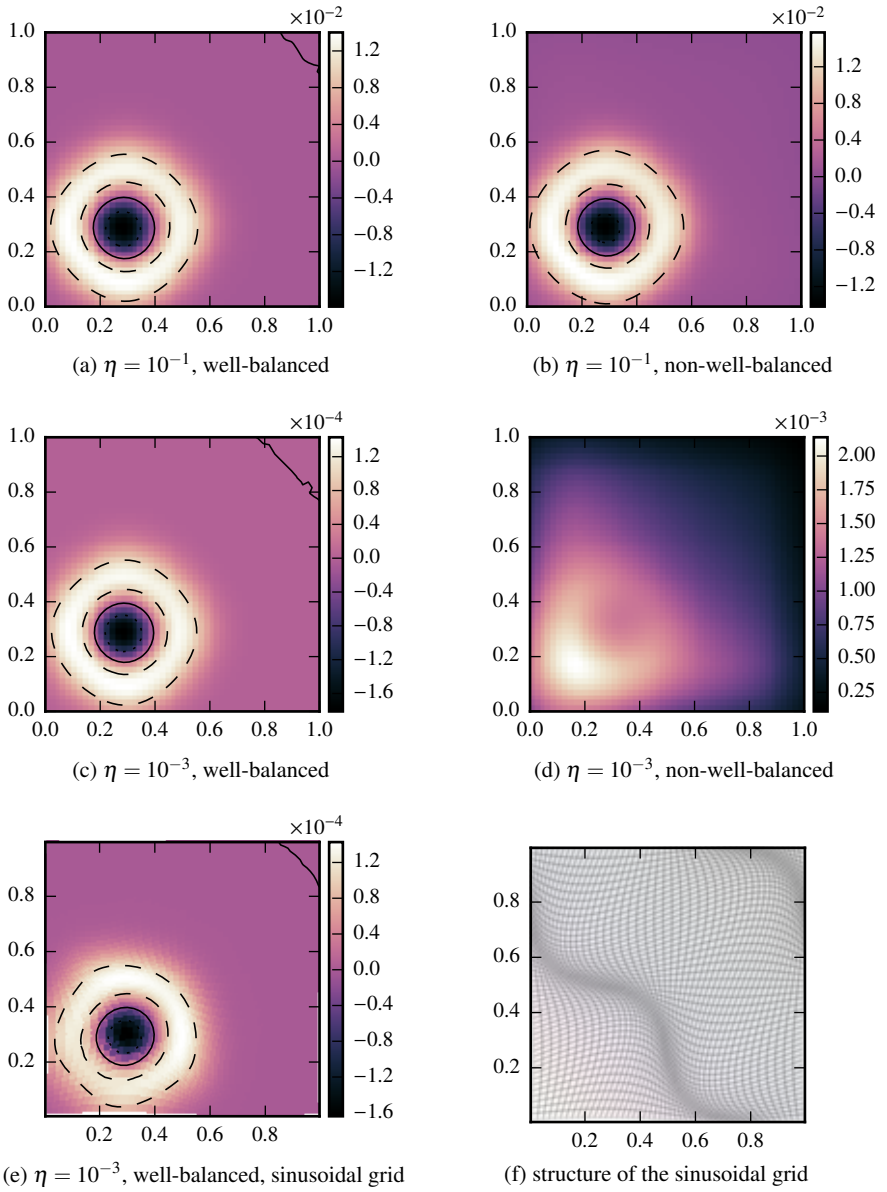

(a) $\eta = 10^{-1}$, well-balanced

(b) $\eta = 10^{-1}$, non-well-balanced

(c) $\eta = 10^{-3}$, well-balanced

(d) $\eta = 10^{-3}$, non-well-balanced

(e) $\eta = 10^{-3}$, well-balanced, sinusoidal grid

(f) structure of the sinusoidal grid

Fig. 2: Evolution of a small pressure perturbation on an isothermal equilibrium (Lines: dotted at -0.1η, solid at 0.0, dashed at 0.1η).

8. Shu, Chi-Wang, and Stanley Osher. “Efficient implementation of essentially non-oscillatory shock-capturing schemes.” Journal of Computational Physics 77.2 (1988): 439-471

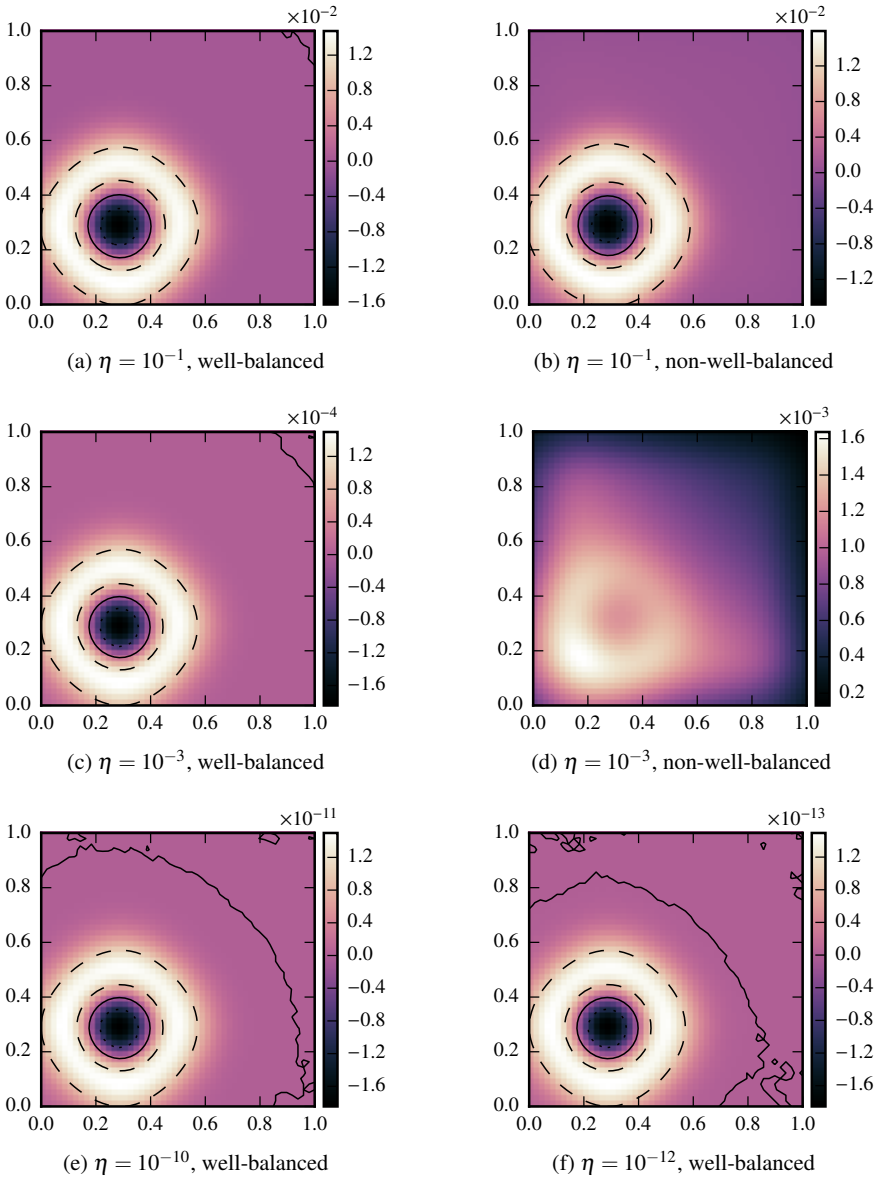

(a) $\eta = 10^{-1}$, well-balanced

(b) $\eta = 10^{-1}$, non-well-balanced

(c) $\eta = 10^{-3}$, well-balanced

(d) $\eta = 10^{-3}$, non-well-balanced

(e) $\eta = 10^{-10}$, well-balanced

(f) $\eta = 10^{-12}$, well-balanced

Fig. 3: Evolution of a small pressure perturbation on an polytropic equilibrium (Lines: dotted at -0.1η, solid at 0.0, dashed at 0.1η).

9. Xing, Y. and Shu, C.W., 2013. High order well-balanced WENO scheme for the gas dynamics equations under gravitational fields. Journal of Scientific Computing, 54(2-3), pp.645-662.